ACS Synthetic Biology

pubs.acs.org/synthbio
Research Article

Metabolite-Responsive Control of Transcription by Phase Separation-Based Synthetic Organelles

Published as part of ACS Synthetic Biology special issue "Materials Design by Synthetic Biology".

Carolina Jerez-Longres and Wilfried Weber*

Cite This: https://doi.org/10.1021/acssynbio.4c00633
Read Online

ABSTRACT: Living natural materials have remarkable sensing abilities that translate external cues into functional changes of the material. The reconstruction of such sensing materials in bottom-up synthetic biology provides the opportunity to develop synthetic materials with life-like sensing and adaptation ability. Key to such functions are material modules that translate specific input signals into a biomolecular response. Here, we engineer a synthetic organelle based on liquid−liquid phase separation that translates a metabolic signal into the regulation of gene transcription. To this aim, we engineer the pyruvate-dependent repressor PdhR to undergo liquid−liquid phase separation *in vitro* by fusion to intrinsically disordered regions. We demonstrate that the resulting coacervates bind DNA harboring PdhR-responsive operator sites in a pyruvate dose-dependent and reversible manner. We observed that the activity of transcription units on the DNA was strongly attenuated following recruitment to the coacervates. However, the addition of pyruvate resulted in a reversible and dose-dependent reconstitution of transcriptional activity. The coacervate-based synthetic organelles linking metabolic cues to transcriptional signals represent a materials approach to confer stimulus responsiveness to minimal bottom-up synthetic biological systems and open opportunities in materials for sensor applications.

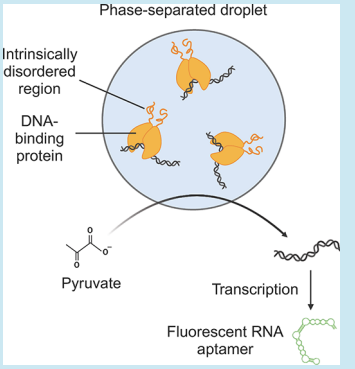

KEYWORDS: *coacervate, intrinsically disordered region, in vitro transcription, liquid−liquid phase separation, repressor protein*

INTRODUCTION

Natural living materials show remarkable features such as stimulus responsiveness or self-organization. Key to stimulus responsiveness of natural materials is the ability of biomolecules to translate external cues such as the concentration of a metabolite into a distinct biochemical output like a change in protein structure, interaction, or enzyme activity. With the emergence of synthetic biology and the ever-growing opportunities of engineering biological systems, it became possible to use such biological receptors to program properties and functions of biological and biohybrid materials.[1−3] For example, the functional coupling of engineered biological receptors to polymers enabled the synthesis of polymer materials that change property and function in response to external cues. Here, the widely occurring mechanism of biological receptors to homo- or heterodimerize in response to an external stimulus has been used to conditionally cross-link (bio-)chemical polymers and thus to change the macroscopic material properties. For example, polymers were cross-linked by receptors that dissociate in response to small-molecule drugs,[4,5] which enabled a dose-dependent dissolution of the resulting material and the release of (therapeutic) biomolecular cargo. More recently, engineered photoreceptors previously used in molecular optogenetics haven been used to cross-link polymers such as polyethylene glycol. With this approach, hydrogel materials have been synthesized that change mechanical properties in a reversible and dose-dependent manner in response to multichromatic light.[6−10]

Similar to the modular design of computational synthetic genetic networks by interconnecting genetic switches, individual biological receptors have been integrated into polymer materials and functionally wired via diffusible signals so that the overall material was able to perform fundamental computational operations such as Boolean algebra, signal amplification, or counting.[11−13] While such materials show high promise as smart sensing devices or as extracellular, dynamically tunable matrix for tissue engineering,[6] programmable biological materials are also key to bottom-up synthetic biology aiming at the assembly of systems with life-like or even living properties. For example, the integration of engineered synthetic biological receptors into biobased or synthetic particles enabled the design of stimulus-responsive cell-like

Received: September 13, 2024
Revised: January 6, 2025
Accepted: January 31, 2025

moieties[14] or the stimulus-inducible assembly and reorganization of synthetic "tissues" from designer protocells.[15−17]

One important process in biological self-assembly and self-organization is based on liquid−liquid phase separation (LLPS), in which biomolecules spontaneously separate in distinct phases. LLPS is the driving mechanism behind the formation of membrane-less organelles such as nucleoli or Cajal bodies that serve as localized biochemical reaction centers.[18] The primary driving forces for the formation of biomolecular condensates are the concentration of the involved molecules (such as proteins, RNA, or DNA), the biophysical properties of the biopolymers involved, and the multivalent interactions among them. Multivalent interaction is often facilitated by intrinsically disordered regions (IDRs), which are sequences of amino acids lacking a defined secondary structure and that can interact via cation−pi, pi-stacking, or electrostatic interactions, for instance.[19,20] Proteins like fused in sarcoma (FUS)[18] and heterogeneous nuclear ribonucleoprotein A1 (HNRNPA1)[21] are well-known examples, as they have been documented to undergo phase separation when a critical concentration threshold is reached. LLPS has emerged as a versatile approach for compartmentalization in bottom-up synthetic biology.[22] For instance, phase-separated compartments that exhibit enzymatic activity have been described.[23−28] In addition, enabled by cell-free synthetic biology technologies,[29] *in vitro* transcription−translation has been achieved in such phase-separated condensates.[30−32]

In this work, we harness the principle of LLPS to assemble synthetic organelles that are able to integrate metabolic signals and to translate these signals into the control of transcription. The synthetic organelles are based on the pyruvate-responsive repressor PdhR engineered to undergo LLPS by fusion to an IDR. We demonstrate that the resulting coacervates can sequester DNA-harboring cognate *pdhO* operator sequences in a pyruvate-dependent manner. We further demonstrate that the sequestration of the DNA correlated with strongly inhibited transcription that was reversible in a dose-dependent manner by the addition of increasing pyruvate concentrations.

The reversible and dose-dependent behavior of these coacervates highlights their potential as dynamic materials for bottom-up synthetic biology, providing a new tool for the regulation of gene expression in response to metabolic signals. Through this work, we aim to advance the understanding of phase-separated systems in bottom-up synthetic biology and pave the way for the development of new materials with applications in biosensing, and beyond.

MATERIAL AND METHODS

Construction of Expression Vectors. The sequences of the nucleic acid constructs used in this study are shown in Table S1. Bacteria with constructs containing more than one *pdhO* repeat were grown at 30 °C to prevent loss of repeats by recombination.

Protein Production and Purification. *Production of 3C Protease.* *Escherichia coli* BL21(DE3)-pLysS cells (Thermo Fisher Scientific, Waltham, Massachusetts, cat. no. C602003) were transformed with plasmid pHJW257,[33] coding for strep-tagged 3CP, and cultivated in Luria/Miller broth (LB) supplemented with ampicillin (100 μg/mL) and chloramphenicol (36 μg/mL). Bacteria were grown in LB medium in flasks at 37 °C while shaking to an OD_{600} of 0.9 prior to induction with 1 mM isopropyl β-D-1-thiogalactopyranoside (IPTG; Carl Roth, Karlsruhe, Germany, cat. no. 2316.5) and a protein production period of 5 h at 37 °C. Subsequently, the bacteria were harvested by centrifugation and the cells were resuspended in column buffer (100 mM Tris−HCl, 150 mM NaCl, pH 8.0, 35 mL per 1 L of initial culture), shock-frozen in liquid nitrogen, and stored at −80 °C until purification. For affinity chromatography purification, resuspended pellets were lysed by ultrasonication (SONOPULS HD, BANDELIN, Berlin, Germany). The lysates were clarified by centrifugation at 30,000*g* for 30 min, and the supernatant was loaded onto a gravity-flow column containing Strep-Tactin XT 4Flow resin (IBA-Lifesciences, Göttingen, Germany, cat. no. 2−5030−002; 1.5 mL StrepTactin beads per 1 L bacterial culture) previously equilibrated with column buffer. The column was washed with 10 column volume (CV) column buffer, after which the protein was eluted in seven fractions of 1 CV each with elution buffer (100 mM Tris−HCl, 150 mM NaCl, 50 mM biotin, pH 8.0). The fractions with the highest absorbance at 280 nm were pooled, and β-mercaptoethanol was added to a final concentration of 10 mM. The eluate was concentrated using a Vivaspin Turbo 5k-molecular weight cutoff (MWCO) spin concentrator (Sartorius AG, Göttingen, Germany, cat. no. VS15T12), and the final concentration was determined by Bradford assay. Finally, 10% (v/v) glycerol was added and the protein was shock-frozen in single-use aliquots in liquid nitrogen and stored at −80 °C.

Production of PdhR and PdhR-FUS$_N$. *E. coli* BL21(DE3) cells (Thermo Fisher Scientific, cat. no. C601003) were transformed with plasmid pRG001 (PdhR)[34] or pCJL236 (MBP-PdhR-FUS$_N$) and selected by growth in Luria/Miller broth (LB) supplemented with ampicillin (100 μg/mL). Precultures were grown overnight and were used to inoculate expression cultures in flasks of LB medium supplemented with ampicillin. The latter were incubated at 37 °C while shaking to an OD_{600} of 0.9 prior to induction with 1 mM IPTG and a protein production period of 4 h at 37 °C. The bacteria were harvested by centrifugation and resuspended in lysis buffer (50 mM NaH_2PO_4, 300 mM NaCl, 10 mM imidazole, pH 8.0; 35 mL per 1 L of initial culture), shock-frozen in liquid nitrogen, and stored at −80 °C until purification. For purification, the pellets were thawed, and 0.5 mM tris(2-carboxyethyl)-phosphine (TCEP) was added. The cells were lysed on an APV 2000 French press (APV Manufacturing, Bydgoszcz, Poland) at 1000 bar. The lysate was clarified by centrifugation at 30,000*g* for 30 min. For PdhR purification, the clarified lysate was loaded onto a gravity-flow column containing a nickel-nitrilotriaceticacid (Ni-NTA) Superflow agarose resin (Qiagen, Hilden, Germany, cat. no. 30410; 1 mL resin per 1 L culture) previously equilibrated with lysis buffer. The column was washed twice with 10 CV wash buffer (50 mm NaH_2PO_4, 300 mm NaCl, 20 mm imidazole, 0.5 mM TCEP, pH 8.0), and the protein was eluted in 8 CV elution buffer (50 mm NaH_2PO_4, 300 mm NaCl, 250 mm imidazole, 0.5 mM TCEP, pH 8.0). The MBP-PdhR-FUS$_N$ protein was purified using an ÄKTA Explorer fast protein liquid chromatography system (GE Healthcare, Freiburg, Germany). The clarified lysate was loaded on a Ni-NTA agarose column, and, after washing with 12 CV wash buffer, elution was carried out in 6 CV elution buffer. The proteins were concentrated using Vivaspin 10k-MWCO spin concentrators (Sartorius AG, cat. no. VS15T02) up to 4 mg/mL (PdhR) and 7 mg/mL (MBP-PdhR-FUS$_N$). Finally, 10% (v/v) glycerol was added and the proteins were

https://doi.org/10.1021/acssynbio.4c00633
ACS Synth. Biol. XXXX, XXX, XXX−XXX

shock-frozen in single-use aliquots in liquid nitrogen and stored at −80 °C.

Formation of PdhR-FUS$_N$ Condensates. MBP-PdhR-FUS$_N$ or PdhR proteins were thawed and desalted into the buffer used for phase separation experiments (10 mM Tris, 150 mM NaCl, pH 7.9) using Zeba spin desalting columns (Thermo Fisher Scientific, cat. no. 89882). $MgCl_2$ was always added to the buffer directly before each experiment to a final concentration of 30 mM. The plasmids coding for SdBroccoli with different *pdhO* repeat configurations were first linearized with the *Xmn*I restriction enzyme, which has one cleavage site per plasmid. The linear DNA was isolated using the Qiagen Gel extraction kit (Qiagen, cat. no. 28704) without previously running a gel, by mixing the digestion mix with the kit's resuspension buffer in the proportions indicated by the manufacturer. The remaining steps were done following the manufacturer's instructions, and the elution was carried out in water. Afterward, the buffer used for phase separation experiments was added from a 10× stock solution. In the experiment shown in Figure 3 and Figure S3, the protein and linearized plasmids (pCJL241) were mixed at 20 μM and 25 nM concentrations, respectively. Na-pyruvate was added where indicated, at the concentration indicated in the figures, and the same volume of buffer was added to samples without pyruvate. The protein, DNA, and pyruvate mixes were incubated for 30 min at 37 °C to allow the DNA and proteins to bind. Afterward, 3C protease was added to a final concentration of 0.1 mg/mL to induce condensate formation, and the samples were incubated for ∼20 h at RT. Subsequently, the samples were prepared for microscopy or *in vitro* transcription, as described below. In experiments shown in Figures 4 and 5and Figures S4 and S9, the protein and linearized plasmids (pCJL240, pCJL241, and pCJL244) were mixed at 20 μM and 25 nM concentrations, respectively. The protein and DNA mixes were incubated for 30 min at 37 °C to allow binding, prior to addition of 0.1 mg/mL 3C protease and incubation overnight at RT to induce condensate formation. Afterward, Na-pyruvate or Na-acetate (Figure S4 only) was added at the concentrations indicated in the figures, and the same volume of buffer was added to samples without pyruvate or acetate. The samples were further incubated for 6 h at RT. Finally, the samples were prepared for microscopy or *in vitro* transcription, as described below.

Widefield Fluorescence Microscopy. To evaluate DNA sequestration into condensates, 10^{-4} mg/mL DAPI dye was added to each sample. After a 15 min incubation period, microscopy images were acquired on an Axio Observer microscope (Zeiss, Oberkochen, Germany) in differential interference contrast (DIC) mode, equipped with a Colibri 2 light source (Zeiss), C-Apochromat 40×/1.20 W Korr and Plan-Apochromat 20×/0.80 M27 objectives (Zeiss), and filters for DAPI (excitation: BP 365, emission: BP 447/60-25) and SdBroccoli (excitation: BP 470/40 HQ, emission: BP 530/50) detection. The images shown in Figure S2 were obtained using an EVOS XL digital inverted microscope (Thermo Fisher Scientific) with phase contrast.

In Vitro Transcription. For *in vitro* transcription, a Mastermix was first prepared containing transcription reagents: T7 polymerase (27 U per 100 μL reaction; Promega, Madison, Wisconsin, cat. no. P2077), 1 mM DTT, and 0.5 mM rNTPs (Promega, cat. no. E6000). The reagent concentrations indicated are the final concentrations in the transcription reactions. The reactions were incubated overnight at RT unless indicated otherwise. To measure SdBroccoli RNA aptamer production, 1 mM DFHBI-1T (Bio-Techne, Minneapolis, Minnesota, cat. no. 5610/10) was added and the samples were further incubated for 1 h at RT unless indicated otherwise. Finally, SdBroccoli fluorescence was measured on a SpectraMax iD5 plate reader (Molecular Devices, San Jose, California) using an excitation wavelength of 482 nm and detecting emission at 535 nm. The results shown in Figure 5b were normalized using the values in Figure S8 (SdBroccoli fluorescence of transcription reactions with DNA alone at different pyruvate concentrations), in order to correct for the differences in transcription levels due to the different ionic strengths of the pyruvate-containing samples.

Software. Acquisition of fluorescence microscopy images was done using ZENblue 3.3 (Zeiss) software. All images were analyzed using FiJi.[35] Quantification of mean fluorescence intensity inside condensates (Figure 3b and Figure S5) was done using FiJi, as follows. First, the DIC images were used to delimitate the regions of the images occupied by condensates. The contrast of the images was enhanced, and a Kuwahara or minimum filter was applied where needed to better distinguish the condensates from the background. A threshold was set manually for each image to obtain a binary mask delimitating the condensates. The mask was cleaned up manually using the original DIC image as a guide. Using FiJi's "Analyze particles" tool, the regions of interest containing condensates were defined, excluding regions located on the edges of the image. These regions of interest were used to measure the mean pixel intensity on the raw fluorescence images. The diameter of individual condensates (Figure S6) was measured manually using FiJi's "segment" and "measure" tools. Objects on the edges of the image were excluded, as well as objects that were out of focus, which might cause a bias toward larger condensates that more readily sediment onto the surface. Nonspherical shapes were measured by their shortest axis. These measurements should be taken as an approximation. The graphs in Figures 3b and 5b and Figures S5−S8 were created using OriginPro (version 2024, OriginLab, Northampton, Massachusetts). Statistical analyses were done using OriginPro. *t* tests were made assuming equal variances. Figures 1 and 5a were created using BioRender.com.

RESULTS AND DISCUSSION

To engineer a synthetic organelle with metabolite-responsive transcription control, we combined protein-based LLPS with the metabolite-responsive recruitment of a transcription cassette into the formed coacervate. We hypothesized that DNA recruitment would interfere with transcription, which could be reversed by metabolite-triggered DNA release. The synthetic organelle was formed by inducing LLPS of the pyruvate-responsive repressor protein PdhR[36] via fusion to the N-terminal intrinsically disordered protein domain of fused in sarcoma (FUS$_N$).[37] PdhR was shown to bind DNA constructs harboring its cognate *pdhO* DNA operator. However, in the presence of increasing pyruvate concentrations, the DNA is released in a dose-dependent manner.[36] We added a coding sequence for the green fluorescent RNA aptamer-stabilized dimeric Broccoli (SdBroccoli), as reporter for transcription from the RNA polymerase T7 promoter on the DNA construct.[38] Transcription was initiated by addition of T7 polymerase and NTPs and quantified after supplementation of the SdBroccoli ligand DFHBI-1T, which emits a fluorescence signal upon complexation by the aptamer (Figure 1).

https://doi.org/10.1021/acssynbio.4c00633
ACS Synth. Biol. XXXX, XXX, XXX−XXX

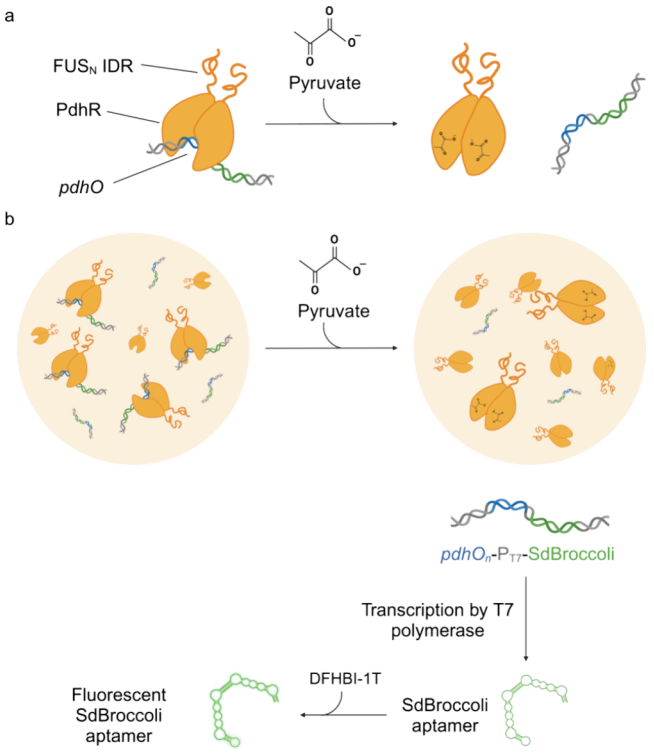

Figure 1. (a) Molecular mechanism of metabolite responsiveness. The bacterial pyruvate dehydrogenase repressor (PdhR) binds to the *pdhO* sequence on a DNA molecule. Upon binding to pyruvate, the protein undergoes a conformational change that prevents it from binding to *pdhO*, therefore releasing the DNA molecule. (b) Design of the liquid−liquid phase separation-based synthetic organelles with metabolite-responsive transcriptional regulation. The pyruvate-responsive repressor protein (PdhR) is fused to the N-terminal intrinsically disordered region (IDR) of the fused in sarcoma protein (FUS_N), which causes the protein to undergo liquid−liquid phase separation. PdhR recruits a DNA molecule containing the cognate *pdhO* operator, which results in transcriptional inhibition of promoters contained on the DNA molecule. However, the addition of pyruvate triggers the reversible and dose-dependent release of the DNA from the coacervate, which results in transcription activity from the T7 promoter. Transcription is quantified by production of the SdBroccoli RNA aptamer binding to its ligand DFHBI-1T.

Construction of the System Components. First, we designed a PdhR fusion protein so that phase separation of the protein could be induced. For that purpose, the FUS IDR was fused at the C terminus of PdhR so as not to interfere with the N-terminal DNA-binding domain. To facilitate production of PdhR-FUS_N in soluble form, we added the maltose-binding protein (MBP) solubility tag to the N-terminus separated by a 3C protease (3CP) cleavage site for later MPB removal and induction of phase separation. As control, a construct encoding PdhR alone was used. Both constructs further contained a hexahistidine tag for purification (Figure 2a). The constructs were produced in *E. coli* and purified by immobilized metal affinity chromatography (Figure S1a,b). The FUS_N-containing construct was subjected to 3CP treatment (Figure S1c) to induce phase separation. After incubation overnight, phase separation was observed with round droplets in sizes ranging from 1 to 10 μm (Figure 2b). Compared to FUS_N alone, PdhR-FUS_N forms larger, round-shaped condensates at higher protein concentrations, with FUS_N forming condensate clusters and eventually aggregates at lower molar concentrations (Figure S2). We therefore expect the PdhR-FUS_N fusion protein to have a higher threshold concentration for phase separation than FUS_N alone. This is in line with previous observations from the fusion of IDRs with a soluble, globular protein.[39,40]

Second, we designed DNA constructs to be recruited into PdhR-FUS_N condensates. For that purpose, one or six repeats of the 32bp *pdhO* operator were placed upstream of the T7 promoter and the SdBroccoli coding sequence. We further built one construct, which contained six repeats of a truncated, 17 bp *pdhO* operator (Figure 2a and Table S1).

Pyruvate-Responsive Recruitment of PdhO-Containing DNA into PdhR-Based Coacervates. We analyzed the recruitment of *pdhO*-containing DNA into PdhR-FUS_N condensates in the presence or absence of pyruvate. For that purpose, MBP-PdhR-FUS_N was mixed with the construct containing one *pdhO* repeat (pCJL241) in the presence or absence of 100 mM Na-pyruvate. After incubation to allow for DNA and protein binding, 3CP was added to cleave the MBP tag and induce condensate formation. After incubation overnight, the samples were stained with DAPI to visualize DNA localization. The samples were analyzed under a fluorescence microscope with DIC. As can be seen in Figure 3a and Figure S3, in the absence of pyruvate, the DAPI signal colocalizes with the condensates, whereas in the presence of 100 mM pyruvate, no colocalization was observed. To quantitatively analyze this effect, we measured the mean fluorescence intensity inside the regions of the images delimitated by condensates (Figure 3b). To rule out that this effect was unspecific, e.g., due to the higher salt concentration of the pyruvate-containing sample, a control was performed with sodium acetate at the same concentration. Under these conditions, colocalization was also observed (Figure S4), showing that the binding and release of the DNA was specific to pyruvate.

Reversibility and Dose Dependency of PdhO DNA Recruitment into PdhR-Based Coacervates. Having demonstrated metabolite-responsive transcription control by protein coacervates, we next evaluated the dose dependency as well as reversibility of this effect. To this aim, we incubated the DNA constructs with different *pdhO* configurations with MBP-PdhR-FUS_N and removed the MBP tag by 3CP treatment to induce phase separation. After incubation overnight, pyruvate was added at increasing concentrations. After incubation for 6 h, DAPI was added and the samples were analyzed by fluorescence microscopy with DIC. For the construct with six *pdhO* repeats, only partial release of the DNA was observed whereas the configuration with one single *pdhO* operator resulted in strong release at pyruvate concentrations of 50 and 100 mM, thus confirming reversibility of the recruitment (Figure 4). Additionally, we quantified the mean fluorescence intensity in the regions of the images delimitated by condensates (Figure S5), corroborating the dose dependency of DNA release at increasing pyruvate concentrations for the DNA molecule with a single *pdhO* repeat (Figure S5a).

Of note, the synthetic organelles in Figure 4 form clusters, with variations in the size and number of both the individual condensates and the clusters. We observe that the synthetic organelles containing a DNA molecule with more *pdhO* repeats (pCJL244 and pCJL240) form more clusters, while the DNA molecule with one *pdhO* sequence (pCJL241) gives rise to slightly larger, less abundant condensates and fewer clusters (Figure S6). This could be explained by previous observations

https://doi.org/10.1021/acssynbio.4c00633
ACS Synth. Biol. XXXX, XXX, XXX−XXX

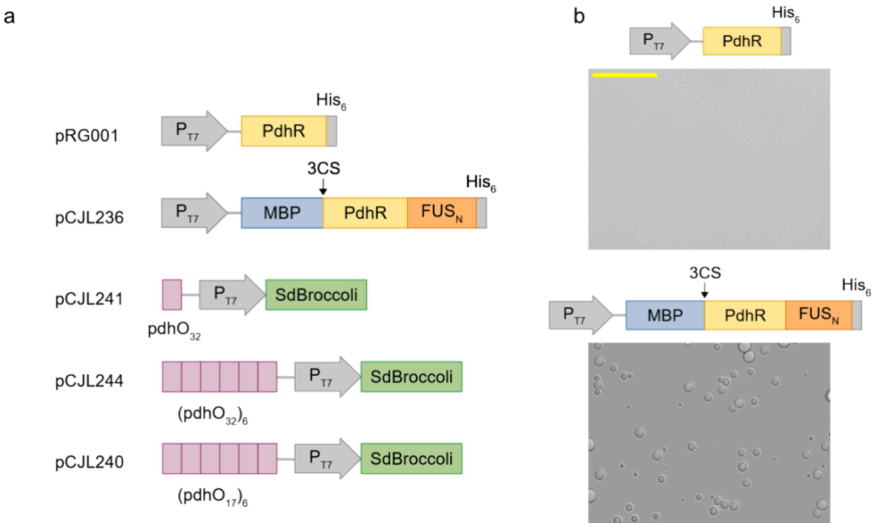

Figure 2. (a) Design of the constructs. Expression vectors for PdhR. The gene encoding PdhR was fused to the N-terminal intrinsically disordered region of FUS (FUS_N). To ensure solubility of the protein during production, a sequence encoding the highly soluble maltose-binding protein (MBP) was fused upstream of PdhR separated by the coding sequence for a cleavage site for 3C protease (3CS). The constructs further contained a hexahistidine tag (His_6) for purification. DNA constructs for coacervate-recruitment-responsive transcription. One (pCJL241) or six (pCJL244) repeats of the *pdhO* operator (32 bp each) were cloned upstream a T7 promoter followed by a sequence encoding the SdBroccoli aptamer. Additionally, a construct containing six truncated *pdhO* operators (17 bp each) was constructed (pCJL240). For a more detailed description of the plasmids and sequence details, see Table S1. (b) Coacervate formation of PdhR-FUS_N. 20 μM MPB-PdhR-FUS_N was incubated with 3C protease to remove solubility promoting MBP prior to analysis by phase-contrast microscopy (bottom panel). As control, a solution containing 20 μM PdhR (top panel) was used. Scale bar = 50 μm.

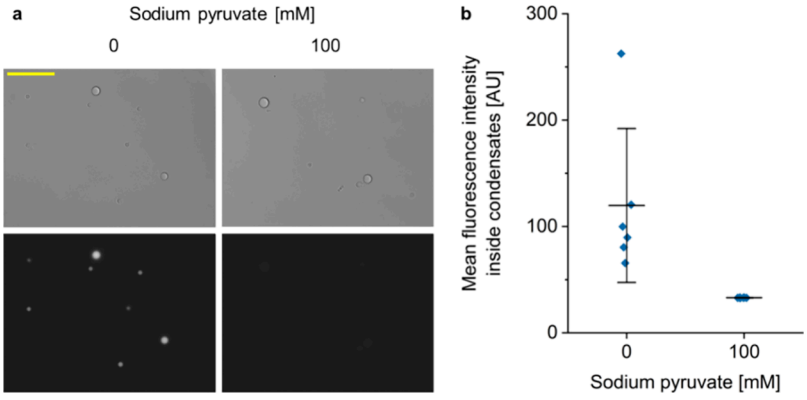

Figure 3. Pyruvate-responsive recruitment of *pdhO*-containing DNA into PdhR-based coacervates. 20 μM MBP-PdhR-FUS_N was mixed with 25 nM linear DNA encoding *pdhO*-P_{T7}-SdBroccoli (pCJL241) for 30 min in the presence or absence of 100 mM pyruvate. 3C protease was added overnight to remove the MBP solubility tag and to induce coacervate formation. (a) DNA was visualized by DAPI staining, and the samples were analyzed by DIC (upper panels) and fluorescence microscopy (lower panels). Scale bar = 50 μm. (b) Quantification of the mean fluorescence intensity in regions delimitated by condensates in the presence or absence of pyruvate. Error bars represent standard deviation. The images used for quantification are shown in Figure 3a and Figure S3.

that a higher multivalency of interactions among the phase separating molecules results in stiffer condensates,[41,42] which may result in the loss of properties such as the ability to coalesce upon contact.[21,37,43,44] Additionally, differences in cluster formation were also observed under different pyruvate concentrations, suggesting that the material properties of the synthetic organelles change depending on their DNA content.

Reversible and Dose-Dependent Transcriptional Modulation By Pyruvate-Responsive Recruitment into Coacervates. To investigate whether the pyruvate-responsive reversible DNA recruitment also correlated with reversible transcription activity from the recruited DNA, we formed coacervates containing the DNA construct with one *pdhO* operator and added increasing concentrations of pyruvate similarly to the experiment in Figure 4. After addition of T7 RNA polymerase and NTPs, transcription was performed overnight prior to the addition of the SdBroccoli ligand DFHBI-1T and fluorescence measurement (Figure 5). We observed a strong drop in transcription activity in the presence of DNA-recruiting coacervates in comparison to free DNA (Figure 5b) but also in comparison to a buffer containing noncoacervate forming PdhR at the same molar concentration as PdhR-FUS_N (Figure 5b and Figure S7). This confirms that recruitment into the condensate rather than the binding of PdhR alone causes transcriptional downregulation. In the presence of increasing pyruvate concentrations, however, a stepwise increase in SdBroccoli fluorescence was observed indicating that the reversible release of DNA from the coacervates correlated with a dose-dependent recovery of transcriptional activity. This data confirms the hypothesis that

https://doi.org/10.1021/acssynbio.4c00633
ACS Synth. Biol. XXXX, XXX, XXX−XXX

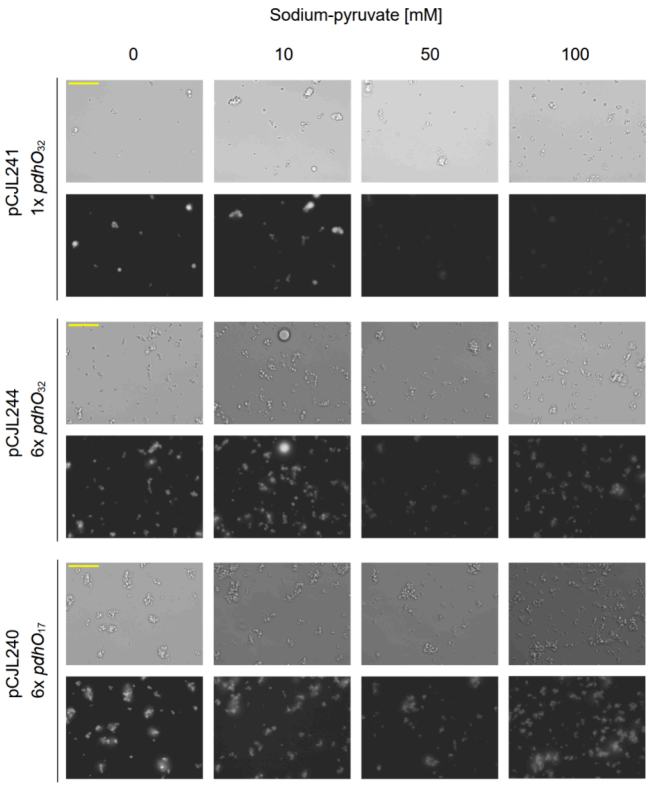

Figure 4. Pyruvate-reversible recruitment of *pdhO*-DNA by PdhR-FUS_N condensates. Linear DNA constructs with different numbers and variants of *pdhO* operators (25 nM each, see Figure 2a) were mixed with 20 μM MBP-PdhR-FUS_N prior to addition of 3C protease to induce coacervate formation by removal of the MBP tag. After incubation overnight, increasing concentrations of pyruvate were added. After 6 h of incubation, the samples were DAPI-stained and analyzed by DIC (upper panels) and fluorescence microscopy (lower panels). Scale bar = 50 μm.

recruitment of the DNA construct into the coacervate-based synthetic organelles correlates with downregulation of transcription and that transcription can be recovered by the metabolite-responsive release in a reversible and dose-dependent manner.

Additionally, we analyzed the localization of SdBroccoli after *in vitro* transcription under fluorescence microscopy and observed SdBroccoli fluorescence inside condensates in the absence of pyruvate, indicating the presence of transcripts also within the condensates (Figure S9).

CONCLUSION AND OUTLOOK

In this study, we have developed synthetic organelles, based on phase separation of a DNA-binding protein fused with an IDR, that are able of recruiting or releasing a DNA molecule in response to the absence or presence of a metabolite, and to control one of the key functions in living systems—transcription of a gene. Even though transcription-regulating phase-separated synthetic organelles have already been achieved by others,[30−32] this is the first example in which the activity of the synthetic organelles can be regulated by a metabolite. This opens up new venues of research, such as combining the transcription-regulating synthetic organelles with other phase separation-based organelles, such as those with enzymatic activity,[24−28] which have already been described. Ultimately, this could lead to the engineering of a fully synthetic protocell with various organelles, each performing a different function. Furthermore, the pyruvate-responsive synthetic organelle described here can be seen as blueprint for the design of synthetic organelles responsive to a broad palette of input molecules such as different metabolites, drugs, or heavy metals by replacing PdhR with a repressor protein-responsive to one of these compound classes.[45,46] The synthetic organelle approach described here may not only be instrumental for bottom-up synthetic biology in conferring minimal cells with sensing and actuation capacity but also open

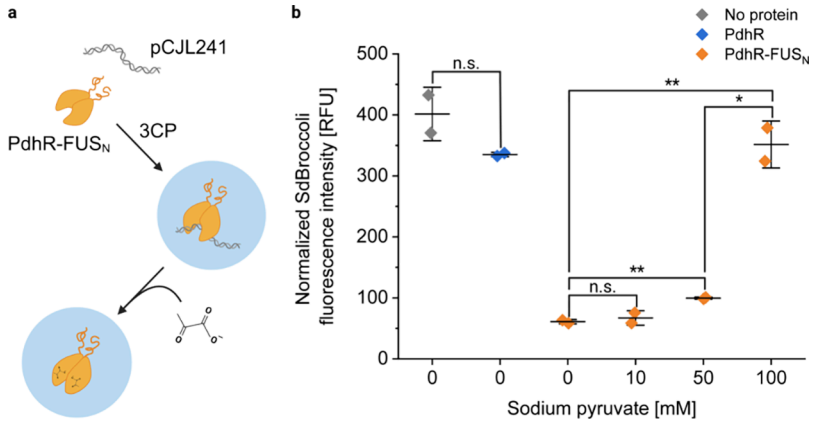

Figure 5. Reversible and dose-dependent control of transcription by pyruvate-responsive recruitment of DNA into PdhR-FUS_N coacervates. (a) MBP-PdhR-FUS_N (20 μM) and a linear DNA construct (25 nM, pCJL241) encoding one *pdhO* operator upstream the T7-promoter-driven SdBroccoli expression cassette were mixed and incubated overnight in the presence of 3C protease to induce coacervate formation. Pyruvate was added at 10, 50, or 100 mM concentration followed by another 6 h incubation. Subsequently, T7 polymerase and NTPs were added. After incubation overnight at RT, the SdBroccoli ligand DFHBI-1T was added and fluorescence was measured after 1 h. (b) SdBroccoli fluorescence intensity after transcription of DNA recruited into PdhR-FUS_N coacervates at increasing pyruvate concentrations. As controls, samples without any proteins and with PhdR alone were included. To correct for the differences in transcription levels due to different ionic strengths of the pyruvate-containing samples, transcription reactions with DNA alone in the presence of respective pyruvate concentrations were carried out (Figure S8), and their SdBroccoli fluorescence levels were used to normalize the results shown here. Error bars represent standard deviation. These results are representative of two independent experiments. The asterisks indicate statistical significance with with a *p*-value of <0.05 (*) or <0.01 (**); n.s. = not significant.

https://doi.org/10.1021/acssynbio.4c00633
ACS Synth. Biol. XXXX, XXX, XXX−XXX

new avenues in the construction of modular sensor materials for specifically detecting biomedical and environmentally important analytes.

■ ASSOCIATED CONTENT

Supporting Information

The Supporting Information is available free of charge at https://pubs.acs.org/doi/10.1021/acssynbio.4c00633.

Relevant DNA sequences of all plasmids generated in this study (Table S1), protein purification steps (Figure S1), fluorescence images of phase separation experiments with the proteins used in this study under varying conditions (Figures S2−S4 and Figure S9), results of fluorescence image quantifications (Figures S5 and S6), and supporting experiments for SdBroccoli fluorescence after *in vitro* transcription reactions (Figures S7 and S8) (PDF)

■ AUTHOR INFORMATION

Corresponding Author

Wilfried Weber − *INM − Leibniz Institute for New Materials, 66123 Saarbrücken, Germany; Department of Materials Science and Engineering, Saarland University, 66123 Saarbrücken, Germany; Signalling Research Centers BIOSS and CIBSS, Faculty of Biology, and SGBM - Spemann Graduate School of Biology and Medicine, University of Freiburg, 79104 Freiburg, Germany;* orcid.org/0000-0003-4340-4446; Email: wilfried.weber@leibniz-inm.de

Author

Carolina Jerez-Longres − *INM − Leibniz Institute for New Materials, 66123 Saarbrücken, Germany; Signalling Research Centers BIOSS and CIBSS, Faculty of Biology, and SGBM - Spemann Graduate School of Biology and Medicine, University of Freiburg, 79104 Freiburg, Germany*

Complete contact information is available at: https://pubs.acs.org/10.1021/acssynbio.4c00633

Author Contributions

Carolina Jerez-Longres: conceptualization; planning, execution, and analysis of experiments; writing—original draft; and figure preparation. Wilfried Weber: conceptualization; funding acquisition; writing—review and editing; and planning and analysis of experiments.

Notes

The authors declare no competing financial interest.

■ REFERENCES

(1) Burgos-Morales, O.; Gueye, M.; Lacombe, L.; Nowak, C.; Schmachtenberg, R.; Hörner, M.; Jerez-Longres, C.; Mohsenin, H.; Wagner, H. J.; Weber, W. Synthetic biology as driver for the biologization of materials sciences. *Mater. Today Bio* **2021**, *11*, No. 100115.

(2) Gharios, R.; Francis, R. M.; DeForest, C. A. Chemical and biological engineering strategies to make and modify next-generation hydrogel biomaterials. *Matter* **2023**, *6*, 4195−4244.

(3) Jakobus, K.; Wend, S.; Weber, W. Synthetic mammalian gene networks as a blueprint for the design of interactive biohybrid materials. *Chem. Soc. Rev.* **2012**, *41*, 1000−1018.

(4) Ehrbar, M.; Schoenmakers, R.; Christen, E. H.; Fussenegger, M.; Weber, W. Drug-sensing hydrogels for the inducible release of biopharmaceuticals. *Nat. Mater.* **2008**, *7*, 800−804.

(5) Christen, E. H.; Karlsson, M.; Kämpf, M. M.; Schoenmakers, R.; Gübeli, R. J.; Wischhusen, H. M.; Friedrich, C.; Fussenegger, M.; Weber, W. Conditional DNA-Protein Interactions Confer Stimulus-Sensing Properties to Biohybrid Materials. *Adv. Funct. Mater.* **2011**, *21*, 2861−2867.

(6) Hörner, M.; Raute, K.; Hummel, B.; Madl, J.; Creusen, G.; Thomas, O. S.; Christen, E. H.; Hotz, N.; Gübeli, R. J.; Engesser, R.; Rebmann, B.; Lauer, J.; Rolauffs, B.; Timmer, J.; Schamel, W. W. A.; Pruszak, J.; Römer, W.; Zurbriggen, M. D.; Friedrich, C.; Walther, A.; Minguet, S.; Sawarkar, R.; Weber, W. Phytochrome-Based Extracellular Matrix with Reversibly Tunable Mechanical Properties. *Adv. Mater.* **2019**, *31*, No. 1806727.

(7) Liu, L.; Shadish, J. A.; Arakawa, C. K.; Shi, K.; Davis, J.; DeForest, C. A. Cyclic Stiffness Modulation of Cell-Laden Protein−Polymer Hydrogels in Response to User-Specified Stimuli Including Light. *Adv. Biosyst.* **2018**, *2*, No. 1800240.

(8) Zhang, X.; Dong, C.; Huang, W.; Wang, H.; Wang, L.; Ding, D.; Zhou, H.; Long, J.; Wang, T.; Yang, Z. Rational design of a photoresponsive UVR8-derived protein and a self-assembling peptide-protein conjugate for responsive hydrogel formation. *Nanoscale* **2015**, *7*, 16666−16670.

(9) Wang, R.; Yang, Z.; Luo, J.; Hsing, I. M.; Sun, F. B12-dependent photoresponsive protein hydrogels for controlled stem cell/protein release. *Proc. Natl. Acad. Sci. U. S. A.* **2017**, *114*, 5912−5917.

(10) Månsson, L. K.; Pitenis, A. A.; Wilson, M. Z. Extracellular Optogenetics at the Interface of Synthetic Biology and Materials Science. *Front. Bioeng. Biotechnol.* **2022**, *10*, No. 903982.

(11) Wagner, H. J.; Engesser, R.; Ermes, K.; Geraths, C.; Timmer, J.; Weber, W. Synthetic biology-inspired design of signal-amplifying materials systems. *Mater. Today* **2019**, *22*, 25−34.

(12) Badeau, B. A.; Comerford, M. P.; Arakawa, C. K.; Shadish, J. A.; Deforest, C. A. Engineered modular biomaterial logic gates for environmentally triggered therapeutic delivery. *Nat. Chem.* **2018**, *10*, 251−258.

(13) Beyer, H. M.; Engesser, R.; Hörner, M.; Koschmieder, J.; Beyer, P.; Timmer, J.; Zurbriggen, M. D.; Weber, W. Synthetic Biology Makes Polymer Materials Count. *Adv. Mater.* **2018**, *30*, No. 1800472.

(14) Ji, Y.; Chakraborty, T.; Wegner, S. V. Self-Regulated and Bidirectional Communication in Synthetic Cell Communities. *ACS Nano* **2023**, *17*, 8992−9002.

(15) Sentürk, O. I.; Chervyachkova, E.; Ji, Y.; Wegner, S. V. Independent Blue and Red Light Triggered Narcissistic Self-Sorting Self-Assembly of Colloidal Particles. *Small* **2019**, *15*, No. 1901801.

(16) Heidari, A.; Sentürk, O. I.; Yang, S.; Joesaar, A.; Gobbo, P.; Mann, S.; de Greef, T. F. A.; Wegner, S. V. Orthogonal Light-Dependent Membrane Adhesion Induces Social Self-Sorting and Member-Specific DNA Communication in Synthetic Cell Communities. *Small* **2023**, *19*, No. 2206474.

(17) Mueller, M.; Rasoulinejad, S.; Garg, S.; Wegner, S. V. The Importance of Cell-Cell Interaction Dynamics in Bottom-Up Tissue Engineering: Concepts of Colloidal Self-Assembly in the Fabrication of Multicellular Architectures. *Nano Lett.* **2020**, *20*, 2257−2263.

(18) Bracha, D.; Walls, M. T.; Brangwynne, C. P. Probing and engineering liquid-phase organelles. *Nat. Biotechnol.* **2019**, *37*, 1435−1445.

(19) Shin, Y.; Brangwynne, C. P. Liquid phase condensation in cell physiology and disease. *Science* **2017**, *357*, No. eaaf4382.

(20) Banani, S. F.; Lee, H. O.; Hyman, A. A.; Rosen, M. K. Biomolecular condensates: Organizers of cellular biochemistry. *Nat. Rev. Mol. Cell. Biol.* **2017**, *18*, 285−298.

(21) Molliex, A.; Temirov, J.; Lee, J.; Coughlin, M.; Kanagaraj, A. P.; Kim, H. J.; Mittag, T.; Taylor, J. P. Phase Separation by Low Complexity Domains Promotes Stress Granule Assembly and Drives Pathological Fibrillization. *Cell* **2015**, *163*, 123−133.

(22) Martin, N. Dynamic synthetic cells based on liquid−liquid phase separation. *ChemBioChem.* **2019**, *20*, 2553−2568.

(23) Zhao, E. M.; Suek, N.; Wilson, M. Z.; Dine, E.; Pannucci, N. L.; Gitai, Z.; Avalos, J. L.; Toettcher, J. E. Light-based control of

metabolic flux through assembly of synthetic organelles. *Nat. Chem. Biol.* **2019**, *15*, 589−597.
(24) Küffner, A. M.; Prodan, M.; Zuccarini, R.; Capasso Palmiero, U.; Faltova, L.; Arosio, P. Acceleration of an enzymatic reaction in liquid phase separated compartments based on intrinsically disordered protein domains. *ChemSystemsChem.* **2020**, *2*, No. e2000001.
(25) Testa, A.; Dindo, M.; Rebane, A. A.; Nasouri, B.; Style, R. W.; Golestanian, R.; Dufresne, E. R.; Laurino, P. Sustained enzymatic activity and flow in crowded protein droplets. *Nat. Commun.* **2021**, *12*, 6293.
(26) Modi, N.; Chen, S.; Adjei, I. N. A.; Franco, B. L.; Bishop, K. J. M.; Obermeyer, A. C. Designing negative feedback loops in enzymatic coacervate droplets. *Chem. Sci.* **2023**, *14*, 4735−4744.
(27) Mason, A. F.; Buddingh', B. C.; Williams, D. S.; van Hest, J. C. M. Hierarchical Self-Assembly of a Copolymer-Stabilized Coacervate Protocell. *J. Am. Chem. Soc.* **2017**, *139*, 17309−17312.
(28) Faltova, L.; Küffner, A. M.; Hondele, M.; Weis, K.; Arosio, P. Multifunctional protein materials and microreactors using low complexity domains as molecular adhesives. *ACS Nano* **2018**, *12*, 9991−9999.
(29) Laohakunakorn, N.; Grasemann, L.; Lavickova, B.; Michielin, G.; Shahein, A.; Swank, Z.; Maerkl, S. J. Bottom-Up Construction of Complex Biomolecular Systems With Cell-Free Synthetic Biology. *Front. Bioeng. Biotechnol.* **2020**, *8*, 213.
(30) Schoenmakers, L. L. J.; Yewdall, N. A.; Lu, T.; André, A. A. M.; Nelissen, F. H. T.; Spruijt, E.; Huck, W. T. S. In vitro transcription-translation in an artificial biomolecular condensate. *ACS Synth. Biol.* **2023**, *12*, 2004−2014.
(31) Sokolova, E.; Spruijt, E.; Hansen, M. M. K.; Dubuc, E.; Groen, J.; Chokkalingam, V.; Piruska, A.; Heus, H. A.; Huck, W. T. S. Enhanced transcription rates in membrane-free protocells formed by coacervation of cell lysate. *Proc. Natl. Acad. Sci. U. S. A.* **2013**, *110*, 11692−11697.
(32) Dora. Tang, T. Y.; van Swaay, D.; deMello, A.; Ross Anderson, J. L.; Mann, S. In vitro gene expression within membrane-free coacervate protocells. *Chem. Commun.* **2015**, *51*, 11429−11432.
(33) Jerez-Longres, C.; Gómez-Matos, M.; Becker, J.; Hörner, M.; Wieland, F. G.; Timmer, J.; Weber, W. Engineering a material-genetic interface as safety switch for embedded therapeutic cells. *Biomater. Adv.* **2023**, *150*, No. 213422.
(34) Ketterer, S.; Hövermann, D.; Guebeli, R. J.; Bartels-Burgahn, F.; Riewe, D.; Altmann, T.; Zurbriggen, M. D.; Junker, B.; Weber, W.; Meier, M. Transcription factor sensor system for parallel quantification of metabolites on-chip. *Anal. Chem.* **2014**, *86*, 12152−12158.
(35) Schindelin, J.; Arganda-Carreras, I.; Frise, E.; Kaynig, V.; Longair, M.; Pietzsch, T.; Preibisch, S.; Rueden, C.; Saalfeld, S.; Schmid, B.; Tinevez, J. Y.; White, D. J.; Hartenstein, V.; Eliceiri, K.; Tomancak, P.; Cardona, A. Fiji: An open-source platform for biological-image analysis. *Nat. Methods* **2012**, *9*, 676−682.
(36) Quail, M. A.; Guest, J. R. Purification, characterization and mode of action of PdhR, the transcriptional repressor of the pdhR-aceEF-lpd operon of Escherichia coli. *Mol. Microbiol.* **1995**, *15*, 519−529.
(37) Patel, A.; Lee, H. O.; Jawerth, L.; Maharana, S.; Jahnel, M.; Hein, M. Y.; Stoynov, S.; Mahamid, J.; Saha, S.; Franzmann, T. M.; Pozniakovski, A.; Poser, I.; Maghelli, N.; Royer, L. A.; Weigert, M.; Myers, E. W.; Grill, S.; Drechsel, D.; Hyman, A. A.; Alberti, S. A liquid-to-solid phase transition of the ALS Protein FUS accelerated by disease mutation. *Cell* **2015**, *162*, 1066−1077.
(38) Alam, K. K.; Tawiah, K. D.; Lichte, M. F.; Porciani, D.; Burke, D. H. A fluorescent split aptamer for visualizing RNA-RNA assembly in vivo. *ACS Synth. Biol.* **2017**, *6*, 1710−1721.
(39) Brumbaugh-Reed, E. H.; Gao, Y.; Aoki, K.; Toettcher, J. E. Rapid and reversible dissolution of biomolecular condensates using light-controlled recruitment of a solubility tag. *Nat. Commun.* **2024**, *15*, 1−13.
(40) Schuster, B. S.; Reed, E. H.; Parthasarathy, R.; Jahnke, C. N.; Caldwell, R. M.; Bermudez, J. G.; Ramage, H.; Good, M. C.; Hammer, D. A. Controllable protein phase separation and modular recruitment to form responsive membraneless organelles. *Nat. Commun.* **2018**, *9*, 2985.
(41) Fischer, A. A. M.; Robertson, H. B.; Kong, D.; Grimm, M. M.; Grether, J.; Groth, J.; Baltes, C.; Fliegauf, M.; Lautenschläger, F.; Grimbacher, B.; Ye, H.; Helms, V.; Weber, W. Engineering Material Properties of Transcription Factor Condensates to Control Gene Expression in Mammalian Cells and Mice. *Small* **2024**, *20*, No. 2311834.
(42) Shin, Y.; Berry, J.; Pannucci, N.; Haataja, M. P.; Toettcher, J. E.; Brangwynne, C. P. Spatiotemporal control of intracellular phase transitions using light-activated optoDroplets. *Cell* **2017**, *168*, 159−171.
(43) Lin, Y.; Protter, D. S. W.; Rosen, M. K.; Parker, R. Formation and Maturation of Phase-Separated Liquid Droplets by RNA-Binding Proteins. *Mol. Cell* **2015**, *60*, 208−219.
(44) Brangwynne, C. P.; Eckmann, C. R.; Courson, D. S.; Rybarska, A.; Hoege, C.; Gharakhani, J.; Jülicher, F.; Hyman, A. A. Germline P granules are liquid droplets that localize by controlled dissolution/condensation. *Science* **2009**, *324*, 1729−1732.
(45) Ramos, J. L.; Martínez-Bueno, M.; Molina-Henares, A. J.; Terán, W.; Watanabe, K.; Zhang, X.; Gallegos, M. T.; Brennan, R.; Tobes, R. The TetR Family of Transcriptional Repressors. *Microbiol. Mol. Biol. Rev.* **2005**, *69*, 326−356.
(46) Cuthbertson, L.; Nodwell, J. R. The TetR Family of Regulators. *Microbiol. Mol. Biol. Rev.* **2013**, *77*, 440−475.

https://doi.org/10.1021/acssynbio.4c00633
ACS Synth. Biol. XXXX, XXX, XXX−XXX